OPTIMUM CONDITIONS OF ICE DESUBLIMATION* UNDER VACUUM AND THEIR EFFECT ON ITS DENSITY AND THERMAL CONDUCTIVITY

D. P. Lebedev and E. F. Andreev

UDC 536.429.4

The mean effective thermal conductivity and the density of ice desublimated under vacuum have been determined experimentally. It is shown that the desublimation rate becomes maximum within the 1.0-2.5 mm Hg pressure range.

Most published data on the desublimation of water vapor under vacuum refer to conditions in industrial or semiindustrial condenser–freezer apparatus [1, 2, 5].

The authors have developed an experimental model with which they were able to solve several problems in test apparatus and procedure design while treating sublimation and desublimation as interdependent processes, namely: by simulating both processes on a specially selected surface, by controlling the direction of water vapor flow, by controlling the desublimation process, by determining the transient heat of desublimation and the thickness of the ice layer in formation, and by continuously measuring the basic thermodynamic parameters which govern the rate and the character of the desublimation process: the total pressure in the vacuum chamber, the partial pressure of water vapor, the temperature of the desublimation surface, etc.

The experimental model was built with acrylic glass, making it possible to visually observe the desublimation process (Fig. 1). The model included two essential elements: a source of water vapor and an active desublimation surface. The vapor source was a water-filled container 7 with the top part of a permeable porous metal–ceramic material 8 heated from below with an electric heater 9. Ice was sublimating in the pores of the metal–ceramic under vacuum [3] while a vapor stream toward the desublimation surface was generated.

The vapor desublimator 14 was a cylindrical vessel whose lower part 1 comprised the test segment and whose desublimation was kept cold by means of a refrigerant mixture driven by a special-purpose pump. The flow of vapor was directed from the permeable plate 8 through diaphragms 3 to the desublimation surface 1. At that time the ice layer on the desublimation surface was steadily building up in the direction toward the vapor stream.

The quantity of heat generated during desublimation over a definite time period was measured with a thermal flux probe 2, backed up by temperature measurements with thermocouples (1), (2), (3) in the copper plate 1. The temperature at various points along the height of the forzen ice layer was measured with thermocouples (6), (7), (8), (9). The saturation temperature of water vapor in the model at a given rarefaction level was measured with thermocouple (5). The circled numbers of the diagram denote the respective thermocouple locations. All thermocouple readings were recorded through potentiometers R-307 and ÉPP-09.

The vacuum level inside the model was measured and maintained with a model FA-160 Leybold–Heraeus GmbH vacumeter through a connecting tube 12.

*Desublimation is a phase transformation of a substance directly from vapor to solid state. It is a special case of condensation.

Institute of Chemical Apparatus Design, Moscow. Translated from Inzhenerno-Fizicheskii Zhurnal, Vol. 23, No. 1, pp. 33-41, July, 1972. Original article submitted November 4, 1971.

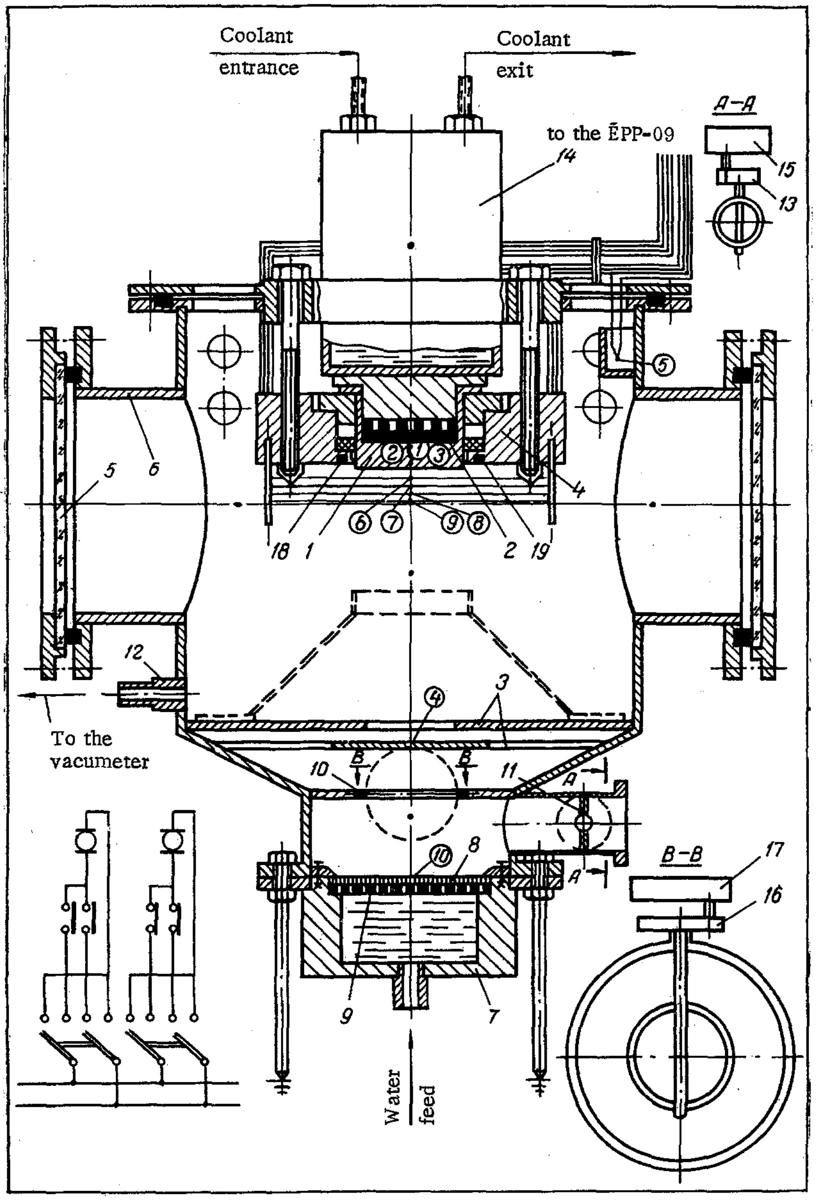

Fig. 1. Experimental model for studying the condensation (desublimation) of water vapor on a flat surface (the circled numbers denote the locations of the thermocouples in the model): 1) desublimation surface; 2) thermal flux probe; 3) diaphragm; 4) plate; 5) window of optical glass; 6) model housing; 7) container for feed water; 8) porous metal plate; 9) heater; 10, 11) gates with an electric drive; 12) connecting pipe for vacuum measurement in the model; 13, 16) speed reducers; 14) coolant tank; 15, 17) motors; 18) protective heater; 19) electric heater.

For studying the transient modes of water vapor desublimation under vacuum we had installed two gates 10 and 11 with electric drives 13-15, 16-17. Before the desired steady state had been reached, the gates were in the positions 10 closed and 11 open for passing vapor from its source to the vacuum chamber. After the desired steady state had been reached, i.e., the temperature of the condensation surface 1 and the vapor flow rate had become steady at the deisred respective levels, gate 10 was opened and gate 11 was closed for passing vapor to the desublimation surface.

In order to prevent vapor from desublimating beyond the active surface of the metal plate 1 (on the adjacent surface), during certain test modes we used in the experimental model a protective heater 18 for holding the temperature of these surfaces near the vapor saturation temperature under the given pressure.

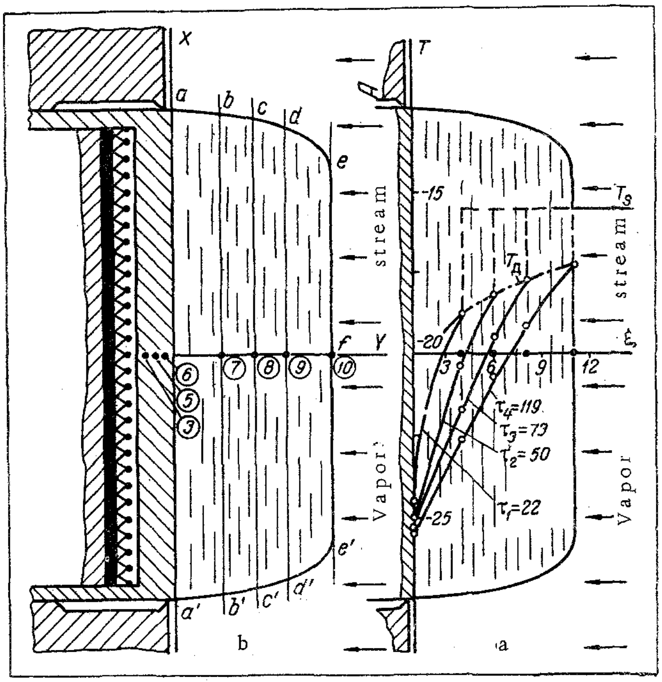

Fig. 2. Goemetry of desublimating ice and the temperature distribution along its thickness: a) temperature distribution along the thickness of a desublimating ice layer; b) geometry of a desublimating ice layer, T (°C), ξ (mm), τ (min).

In order to facilitate visual as well photographic examination, the experimental model was provided with windows 5 of optical glass. The model was placed inside a vacuum chamber where the total pressure was precisely controlled and the wall temperature was held constant. In all tests the desublimation process was carried on until the fourth thermocouple (No. 9 in Fig. 1, farthest away from the desublimation surface) closed. After the last thermocouple above the surface had closed, the desublimation process was terminated and the ice specimen was defrosted with the electric heater 19 for weighing and for a determination of its geometrical characteristics.

Kinetics of the Temperature Field during Desublimation of Ice under Vaccum. The desublimation of water vapor on a flat surface under vacuum was studied over the pressure range from 20 to 0.05 mm Hg at various vapor flow rates. The variation of the temperature field along the x-coordinate in the desublimating ice (under 0.5 mm Hg pressure) at various instants of time is shown in Fig. 2a, where the temperature is seen to vary appreciably with the thickness of the desublimating ice layer: the temperature at the desublimation front T_D approaches the water vapor saturation temperature T_s.

The effective thermal conductivity and the density of desublimated ice were calculated on the basis of the experimentally found temperature field in the specimen.

Heat Balance and Material Balance. Method of Data Evaluation. Our experimental model made it possible to reduce the heat balance and the material balance as well as the sublimation of ice from a permeable plate to the following process:

$$Q_s(\tau_i) = Q_e\eta + q_R^w = \frac{G_{si} r_n}{\Delta\tau_i}. \qquad (1)$$

The quantity of heat generated during desublimation was

$$Q_d(\tau_i) = b\int_0^{\tau=\tau_i} t_\tau(\tau_i)\,d\tau = \frac{\lambda_M}{\delta}\,(t_1 - t_3)\,\Delta\tau_i = \frac{G_I \cdot r_d}{\Delta\tau_i}. \qquad (2)$$

The density of desublimated ice (at a mean-over-the-thickness temperature) was determined as

TABLE 1. Effective Thermal Conductivity of Desublimated Ice as a Function of the Pressure

P, mm Hg	$\Delta G/\Delta\tau$, g/h	r, kcal/kg	$F(\tau_4)\cdot 10^3$, m^2	$[F(\tau_4)+F(\tau_0)]=F(\tau_m)\cdot 10^3$, m^2	t_d, °C	t_s, °C	$\delta(\tau_4)\cdot 10^3$, m	$\delta(\tau_0)\cdot 10^3$, m	λ, kcal/m·h
0,1	3,103	719,6	1,930	1,330	—21,25	—24,80	10,0	0,5	4,967
0,5	4,023	702,2	2,166	1,448	—15,70	—20,50	11,3	0,5	4,572
1,0	4,500	694,8	1,965	1,347	—12,00	—17,40	10,2	0,5	4,362
1,5	5,501	694,0	2,056	1,393	— 9,25	—16,75	10,3	0,5	4,320
2,0	5,973	687,2	2,047	1,389	— 8,50	—15,55	10,2	0,5	4,298
3,0	2,397	681,8	—	—	—19,35	—27,50	10,4	0,5	—
	3,416	702,2	1,923	1,078	—14,65	—19,40	10,3	0,5	4,590
	3,125	702,2	2,026	1,129	—14,50	—18,95	10,7	0,5	4,504
0,5	4,130	702,2	2,022	1,127	—17,15	—22,65	10,3	0,5	4,585
	2,642	702,2	2,000	1,116	—16,20	—19,70	10,2	0,5	4,606
	4,305	702,2	2,095	1,164	—14,70	—20,80	11,1	0,5	4,513

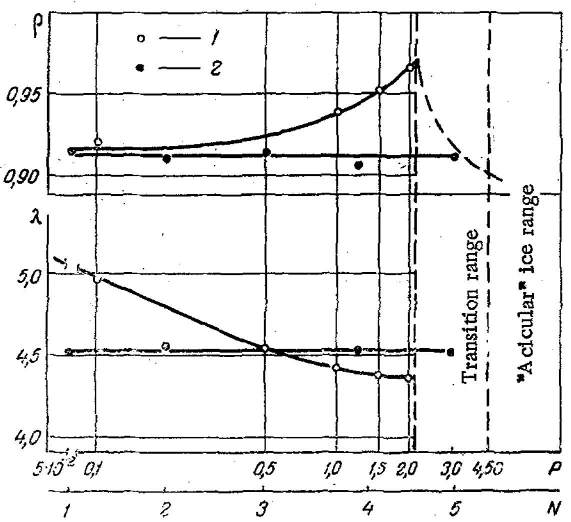

Fig. 3. Density and effective thermal conductivity of desublimated ice as functions of the vacuum level, test No. N at P = 0.5 mm Hg; ρ = f(P) and λ = f(P) (1), ρ = φ(N) and λ = φ(N) (2). Density ρ (g/cm³), conductivity (kcal/m·h·deg C).

$$\rho_I(\bar{T}) = \frac{G_I(\tau_4)}{V_s^* - V_0 - V_\tau} = \frac{G_I(\tau_4)}{\dfrac{\int_a^B x(y)dy}{1+\int_{T_1}^{T_2} \beta(\bar{T})\,dT} - V_0 - V_\tau}, \tag{3}$$

with G_I denoting the mass of desublimated ice, $V_s^* = \int_a^B x(y)dy$ the volume swept by the transformation surface, and function x(y) describing the generatrix curve of the transformation surface plotted from the test coordinates of points *a*, b, c, d, e, f (Fig. 2b).

In all tests function x(y) was obtained by the approximation method and was calculated on a "PROMIN'" computer. The general form of this function was

$$x(y) = A - Be^{-ay} + Ce^{-By}.$$

The nonuniformity of the desublimation surface V_0 was determined by the design characteristics of the model, $V_\beta = \int_{T_1}^{T_2} \beta(\bar{T})dT$ was the volumetric expansion of the ice during the measurement of the geometrical coordinates under atmospheric conditions (with a change in the mean temperature of the desublimated ice volume from the operating temperature $\bar{T}$ to temperature $T_2 \approx -5$°C).

TABLE 2. Density of Desublimated Ice as a Function of the Pressure

$\bar{T}$, °C	P, mm Hg	x (y)	$\int_a^B x dx = V$, cm³	G_I, g	ΔT, °C	$\int_{T_1}^{T_2} \beta T dT$, cm³	V_s^*, cm³	ρ, g/cm²
—22,39	0,1	$22-3,42e^{-0,073y}+9,58e^{-0,485y}$	10,123	7,85	17,40	0,0021	10,1021	0,926
—16,94	0,5	$22-3,32e^{-0,167y}+10,3e^{-0,556y}$	11,544	8,95	11,94	0,0014	11,5282	0,903
—17,08	1,0	$21-11,8e^{-0,428y}+e^{-0,1y}$	10,355	8,19	12,05	0,0014	10,3409	0,939
—11,00	1,5	$22-8,00e^{-0,212y}+4,0e^{-0,965y}$	11,119	9,04	6,00	0,0007	11,1114	0,953
—10,75	2,0	$22-12,4e^{-0,305y}+0$	11,069	9,11	6,00	0,0007	11,0615	0,965
—22,50	3,0	$22,4-16,4e^{-0,535y}+6,0e^{-3,28y}$	11,500	9,38	17,5	0,0021	13,6632	0,95
—16,11	0,5	$22-9,5e^{-0,222y}+6,55e^{-1,167y}$	10,885	8,50	11,11	0,0014	10,8703	0,9187
—18,18	0,5	$22-8,5e^{-0,21y}+3,50e^{-0,750y}$	10,813	8,26	13,18	0,0015	10,7969	0,8999
—16,00	0,5	$21-4,4e^{-0,19y}+8,50e^{-0,650y}$	10,398	7,94	13,00	0,0014	10,3839	0,9058

Note: In all tests V_0 = 1.618 cm³ and V_T = 0.0039 cm³.

The value of thermal expansivity $\beta(\bar{T})$ was taken from [6]. According to calculations, the term V_β could affect the final value of $\rho(\bar{T})$ by not more than ±0.15%. V_T was the volume of thermocouples frozen into the ice.

All parameters in formula (3) were determined at the time $\tau - \tau_4$ (Fig. 2a).

The effective thermal conductivity of desublimated ice was found by the formula

$$\lambda(\tau_4) = \frac{Q(\tau)}{\bar{F}(\tau)} \cdot \frac{\Delta\delta(\tau)}{\Delta t(\tau)} = \frac{2\Delta G(\tau_4)\, r\, d}{\Delta\tau_4} \cdot \frac{[\Delta\delta(\tau_4) + \Delta\delta(\tau_0)]}{[F(\tau_4) + F(\tau_0)]\,[\bar{t}_d(\tau_4) - \bar{t}_s(\tau_4)]}. \tag{4}$$

The magnitude of $\Delta\delta(\tau_0)$ represented the initial thickness of the ice film on the desublimation surface (~0.5 mm).

Test Results. The density and the thermal conductivity of desublimated ice, calculated as functions of the vacuum level according to formulas (3) and (4), are shown in Fig. 3 and in Tables 1 and 2. According to Fig. 3, the density and the thermal conductivity of desublimated ice vary with the vacuum level and differ from those corresponding to atmospheric conditions. The density at −17°C may differ from that of atmospheric ice by 5% and at 2 mm Hg may approach that of water.

The experiment has shown that the entire pressure range covered in this study can, on the basis of the desublimation rate and the forming ice structure, be broken down into three phases corresponding to:

a) acicular ice, 20 mm Hg ≥ P > 4.58 mm Hg;

b) transitional rhombic and pyramidal ice, 4.58 mm Hg > P > 2 mm Hg;

c) laminate-glossy ice, 2 mm Hg > P > 0.05 mm Hg.

Within the 20 mm Hg ≥ P > 4.58 mm Hg range the desublimation process was sluggish, with acicular crystals grown, fractured, and worn away across the entire surface. Within the transition range (above the triple point) the acicular crystals became rhombic and pyramidal. An appreciable increase in the desublimation rate was observed here. As the vacuum dropped below 2 mm Hg, the desublimation surface of ice became smooth and glossy. This surface structure was observed over the entire pressure range from 2 to 0.5 mm Hg. Despite the decreasing density of ice within this range, its thermal conductivity was increasing. This could be explained as a result of two opposing trends: near the triple point, on the one hand, the ice structure appears highly saturated with water, but that water content decreases with decreasing pressure; on the other hand, a decrease in pressure results in a longer free path of molecules within the vapor stream and, therefore, in a lower bond energy of molecules with a consequent lower probability of their condensation (desublimation) where "heeded" on the ice layer surface.

According to Fig. 3, although the ice density stabilizes, the second of these two trends becomes predominant with decreasing pressure, and this explains the increase in the effective thermal conductivity of desublimated ice.

Our results have a tremendous practical significance. Several researchers have pointed out that the sublimation method of drying is probably most efficient under a residual pressure of 1.0-2.5 mm Hg. Our studies confirm and support this proposition. According to Table 1, the desublimation rate $\Delta G/\Delta\tau$ is maximum under a 1.0-2.5 mm Hg vacuum. The sublimation factor as well the desublimation factor are maximum under these conditions.

NOTATION

$Q_s(\tau)$	is the heat supplied for sublimation;
$Q_e\eta = W$	is the power from the electric heater of the permeable plate;
$\Delta G_{si}/\Delta\tau_i$	is the sublimation rate;
r_n	is the heat of evaporation of water;
$Q_d(\tau_i)$	is the heat released by desublimation of water vapor in time τ;
b	is the calibration factor of the thermal flux probe;
$t_T(\tau_i)$	is the reading of the thermal flux probe on the potentiometer;
τ_i	is the desublimation time;
$\Delta\tau_4$	is the time till all thermocouples close;
λ_M	is the thermal conductivity of the active desublimator element;
δ	is the thickness of the active desublimation layer;
$\Delta G_I(\tau_4)/\Delta\tau_4$	is the desublimation rate at the time when all thermocouples are closed with ice;
r_d	is the heat of desublimation;
P	is the total pressure in the model;
$\bar{t}_s$	is the average (over time $\Delta\tau_4$) temperature of the active desublimator surface;
$\bar{t}_d$	is the average (over time $\Delta\tau_4$) temperature of the desublimation front;
$F(\tau_4)$, $F(\tau_0)$	is the surface of desublimated ice at time τ_4 and at time τ_0 respectively;
$\Delta\delta(\tau_4)$, $\Delta\delta(\tau_0)$	is the thickness of desublimated ice layer at time τ_4 and at time τ_0 respectively;
λ_e	is the effective thermal conductivity of desublimated ice;
ρ	is the density of desublimated ice.

LITERATURE CITED

1. A. V. Lykov, Heat and Mass Transfer in Drying Processes [in Russian], Gosénergoizdat (1956).
2. K. P. Shumskii, Principles of Designing Vacuum Sublimation Apparatus [in Russian], Izd. Mashinostroenie (1967).
3. D. P. Lebedev, Izv. VUZ. Énerg., No. 4, 8 (1970).
4. D. P. Lebedev, Abstr. Cand. Dissert., Moskovsk. Inst. Khim. Mashinostr. (1969).
5. L. S. Malkov, Abstr. Cand. Dissert., Leningrad (1970).
6. D. Powell, Physics of Ice [Russian translation], Izd. Mir, Moscow (1966).